SEVERE PLASTIC DEFORMATION

UDC 669.71'3:621.77.016.2:620.18

MECHANISMS OF GRAIN REFINEMENT IN ALUMINUM ALLOYS IN THE PROCESS OF SEVERE PLASTIC DEFORMATION

R. O. Kaibyshev,[1] I. A. Mazurina,[1] and D. A. Gromov[1]

Translated from Metallovedenie i Termicheskaya Obrabotka Metallov, No. 2, pp. 14 – 19, February, 2006.

A study of the mechanisms of grain refinement in the process of severe plastic deformation of two aluminum alloys, i.e., 2219 bearing nanometric particles of Al_3Zr and low-alloy Al – 3% Cu, is described. The alloys are deformed by the method of equal channel angular pressing at 250°C to a maximum strain degree of about 12. The angles of (sub)grain boundaries in alloy 2219 are determined with the help of transmission electron microscopy by the method of Kikuchi lines. The evolution of the microstructure in alloy Al – 3% Cu is studied with the help of grain-boundary maps obtained by the method of electron back-scattered diffraction.

INTRODUCTION

Today, the development of aluminum alloys with ultrafine-grained structure is attracting much practical interest. This is explained by the fact that considerable lowering of the grain size gives many technological advantages and can raise the strength and impact toughness of materials at room temperature [1]. The preferred method for obtaining submicrocrystalline structure in aluminum alloys is a process employing high degrees of deformation without changing the total size of the specimens [2]. The most popular process of treatment of bulk materials by the method of severe plastic deformation (SPD) under laboratory conditions is equal channel angular pressing (ECAP) [2]. Many works have been devoted to the microstructure and mechanical properties of aluminum alloys fabricated by ECAP (for example, [3]). However, the mechanism of grain refinement in pure aluminum and its alloys in the process of ECAP has been studied insufficiently fully [4 – 10]. Moreover, the method of analysis of grain-boundary angles for investigating the evolution of the microstructure at different degrees of deformation has been used in only a few systematic studies [4, 8 – 10]. For this reason, the exact structural mechanism of formation of ultrafine-grained structure in aluminum alloys remains unknown. Two concepts of structural changes that occur in the process of severe plastic deformation in aluminum alloys are preferred.

The authors of [2, 8] assume that at low temperatures the refinement of grains to submicron level in aluminum alloys subjected to ECAP occurs due to the extension and compression of grain boundaries during the deformation and subsequent division of the banded grain structure by transverse large-angle boundaries (LAB) that form in a discontinuous manner. The idea is that this process ensures the main fraction of LAB. The formation of additional strain-induced boundaries plays a less significant role in grain refinement. This mechanism is based on the assumption that the initial grains deform like the entire specimen due to the limited number of active sliding systems.

Another mechanism of grain refinement known as "continuous dynamic recrystallization" (CDR) is suggested in [11], where the authors study the evolution of the microstructure in an Al – Mn alloy in the process of ECAP. The authors of [12, 13] have shown earlier that new grains of nanometric size form in materials with fcc lattice, such as copper and austenitic steels, as a result of a continuous reaction, such as continuous dynamic recrystallization. It has also been shown that CDR causes formation of submicrocrystalline (SMC) grains in aluminum alloys with a high content of dispersoids of nanometric size [14 – 16].

The aim of the present work consisted in studying the mechanisms of refinement of structure in low-alloy aluminum alloy Al – 3% Cu and in dispersoid-containing alloy 2219 in the process of severe plastic deformation at 250°C.

[1] Institute for Problems of Superplasticity of Metals of the Russian Academy of Sciences, Ufa, Russia.

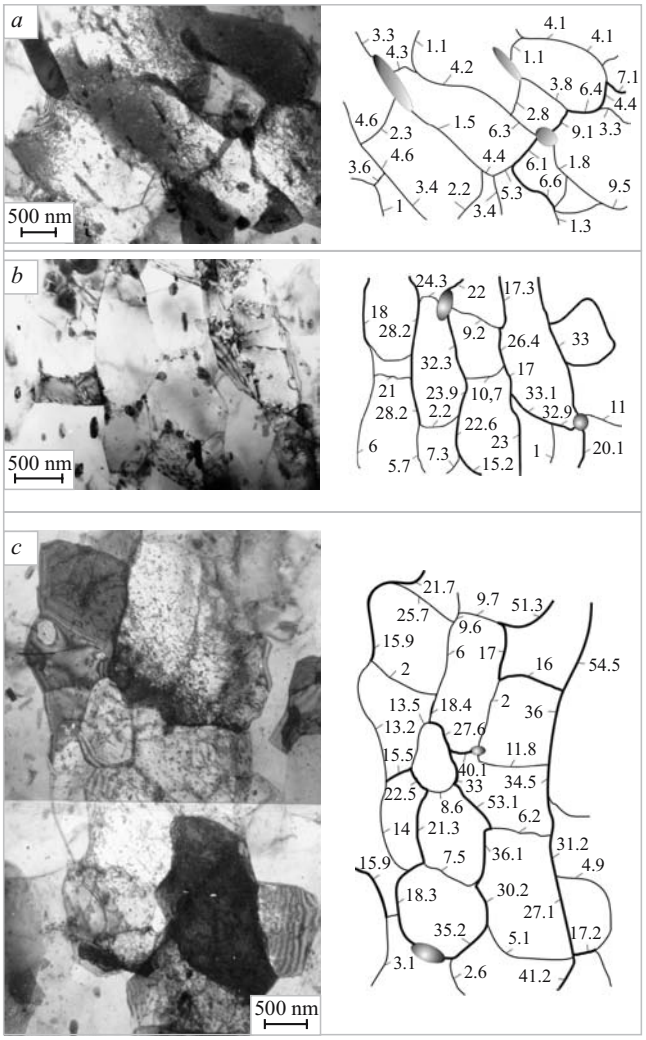

Fig. 1. Microstructures and grain-boundary maps (the numbers present the corresponding grain-boundary angles in degrees) of alloy 2219 deformed by ECAP at 250°C to a true degree of strain ε: *a*) ε = 2; *b*) ε = 4; *c*) ε = 8.

METHODS OF STUDY

Aluminum alloy 2219 (Al – 6.4% Cu – 0.3% Mn – 0.18% Cr – 0.19% Zr – 0.06% Fe) and alloy Al – 3% Cu were obtained by casting into a cooled mold and subsequent homogenizing in two modes, i.e., 530°C, 6 h and 520°C, 4 h. Then both ingots were cut into cylindrical preforms 20 mm diameter and 100 mm long. The initial grain size in alloy 2219 was about 140 μm. The initial structure of alloy Al – 3% Cu was very inhomogeneous; the material contained regions with a mean grain size ranging from about 120 μm to about 450 μm.

ECAP was performed in air in an isothermal die with round-section channel. The channel had an *L* shape. Deformation in such a die ensures a true degree of strain ε ~ 1 in every pass [6]. In order to investigate the formation of the microstructure the preforms were deformed in route A, i.e., after the first pass the preform was withdrawn from the channel and the next pass was made without rotating the preform. Pressing to the required strain degree was conducted without intermediate heating in the furnace. After pressing to ε ~ 1, 2, 4, 8, and 12 the specimens were quenched in water.

After ECAP, a plate was cut from each preform in parallel to the direction of the deformation. The plane of the cut corresponded to the symmetry axis of the plane of the channel [8]. The plate was cut into discs 3 mm in diameter. Then the discs were thinned to about 0.25 mm and subjected to electric polishing in order to remove the deformed surface layer.

Grain-boundary angles in alloy Al – 3% Cu were analyzed by the method of electron back-scattered diffraction (EBSD) using a LEO-1530 attachment (Oxford Instruments, Ltd.) to a scanning electron microscope with spatial resolution of 500 nm and angular resolution of about 0.5°. Randomly chosen regions were scanned at a step of 1 μm. Grain boundaries with angles $\theta \geq 15°$ were treated as large-angle ones and grain boundaries with angles $\theta < 15°$ were treated as small-angle ones.

Analysis of grain-boundary angles in alloy 2219 was made with the help of JEOL-2000EX transmission electron microscope at an accelerating voltage of 160 kV. Discs with a diameter of 3 mm were electropolished until the appearance of a hole in them in a Tenupol-3 installation for jet electropolishing in a solution of 75% CH_3COOH + 25% HNO_3 at $t = -30°C$ and $U = 20$ V. When computing the grain-boundary angles we took into account all well discernible (sub)grain boundaries. The angles of strain-induced boundaries were computed by a standard method of Kikuchi lines [17]. The accuracy of the measurement was about 0.08°. The grain-boundary angles were computed in four randomly chosen regions in each specimen. Altogether we computed about 60 (sub)boundaries in each specimen.

The use of different methods for analyzing grain-boundary angles is explainable by the considerable differences in the microstructure of the alloys, i.e., the presence of a great number of grain boundaries with small angles in alloy Al – 3% Cu made the use of Kikuchi lines difficult.

RESULTS

Alloy 2219. Two types of subgrains form in alloy 2219 at strain degree ε ≤ 2, namely, elongated subgrains alternating with equiaxial subgrains. At deformation with ε ~ 2 individual segments of strain-induced boundaries acquire angles substantially larger than the average grain-boundary angle. Strain-induced boundaries initially have a small-angle misalignment. It can be seen from Fig. 1*a* that a three-dimensional net of small-angle boundaries (SAB) forms in the alloy.

At ε ~ 4 the formation of strain-induced HAB was detected near initial boundaries (Fig. 1*b*). At this degree of deformation we observed mixed SAB and LAB nets. On the whole, the strained structures consisted of elongated crystal-

lites (Fig. 2*a*) that included typical bands arranged in the direction of the displacement.

The majority of longitudinal boundaries arranged in the direction of the displacement initially had large angles, whereas the transverse boundaries had small or medium angles. The average angle of transverse boundaries was about 11° (Fig. 2*b*). It should be noted that strain-induced SAB were located primarily inside the initial grains; in the vicinity of old boundaries the strain-induced boundaries were arranged at large angles.

At a deformation of degree $\varepsilon > 4$ the mean angle of strain-induced boundaries exceeded 15° (Figs. 1*c* and 2*b*). A three-dimensional net of LAB appeared (Fig. 1*c*). At $\varepsilon \sim 8$ we detected recrystallized grains enveloped by LAB on all sides. We also observed crystallites surrounded both by LAB and by SAB. It can be seen that continuous boundaries arranged in the direction of the displacement consist of individual alternating segments with large-angle and small-angle misalignment. We can observe formation of transverse LAB inside elongated (sub)grains (Fig. 1*c*) that acquire an equiaxial shape (Fig. 2*a*). As a result, the average misalignment of the transverse boundaries is less than that of the longitudinal boundaries arranged in the direction of the displacement (Fig. 2*b*). Further deformation increases the proportion of recrystallized grains surrounded by LAB on all sides (Fig. 3). At $\varepsilon \sim 12$ it amounts to almost 85%. The angles of longitudinal LAB increase with growth in the degree of the deformation, whereas the average misalignment of transverse boundaries remains constant (Fig. 2*b*). This is explainable by the permanent formation of transverse SAB inside new grains extended in the direction of the displacement.

Analysis of the data of Fig. 2*a* shows that the size of the (sub)grains has a tendency to reduction with growth in the degree of deformation, which is explainable by division of elongated (sub)grains by transverse SAB. This ensures a decease in the shape factor of the grains determined as the ratio of the grain sizes in the longitudinal and transverse deformation directions, which ensures, on the average, a more equiaxial shape of the new grains (Fig. 2*a*).

It should be noted that the size of the equiaxial crystallites and the distance between the transverse boundaries for deformation of degree $\varepsilon \geq 4$ remain virtually unchanged (Fig. 2*a*). At $\varepsilon \geq 8$ the new grains are elongated in the direction of the displacement. The mean angle θ_m between (sub)grains (Fig. 2*b*) and the number of LAB (Fig. 3) increase at $\varepsilon \geq 2$. It has been shown that at low degrees of deformation the mean grain-boundary angle does not change. In the range of deformation of degree $\varepsilon = 2 - 8$ the data on grain-boundary angles can be approximated by a linear function of accumulated strain having the form $\Delta\theta \propto 5° \times \Sigma\varepsilon$. The mean grain-boundary angle attains the value of apparent saturation at deformation of degree $\varepsilon > \sim 8$ (Fig. 2*b*). The value of the saturation is about 34° (Fig. 2*b*). On the other hand, the number of LAB has a tendency to increase with

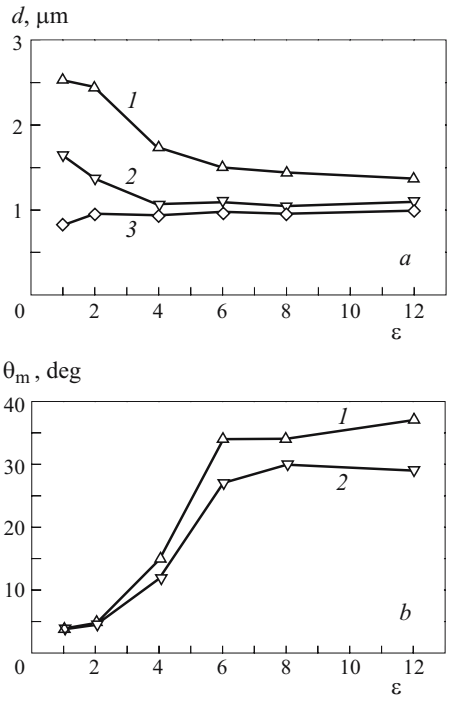

Fig. 2. Dependence of the sizes of crystallites d (*a*) and of the mean angle θ_m of strain-induced boundaries (*b*) on the degree of deformation ($t_{def} = 250°C$) of alloy 2219: *1*, *2*) in longitudinal and transverse deformation directions respectively; *3*) sizes of equiaxial crystallites.

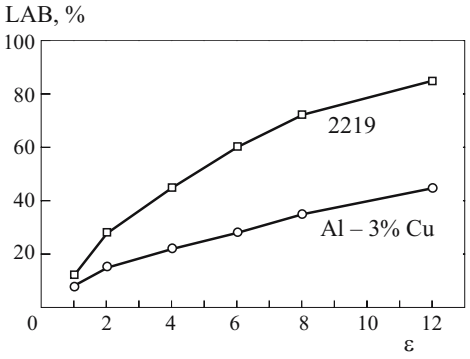

Fig. 3. Fraction of large-angle boundaries (LAB) in the studied alloys as a function of the degree of deformation ε at 250°C.

growth in the degree of the deformation, and at $\varepsilon \sim 12$ it attains about 80%.

Alloy Al – 3% Cu. The results of EBSD analysis of grain-boundary angles in the alloy are presented in Fig. 4. The main distinctive feature of the microstructure of this alloy after the deformation is a high heterogeneity connected with the formation of strain bands surrounded by LAB after the first pass (Fig. 4*a*). In the longitudinal direction the bands have a size of about 400 μm; the visible width of the bands varies from 4 to 40 μm. Numerous transverse SAB with angles ranging from 5 to 10° form inside the bands. A

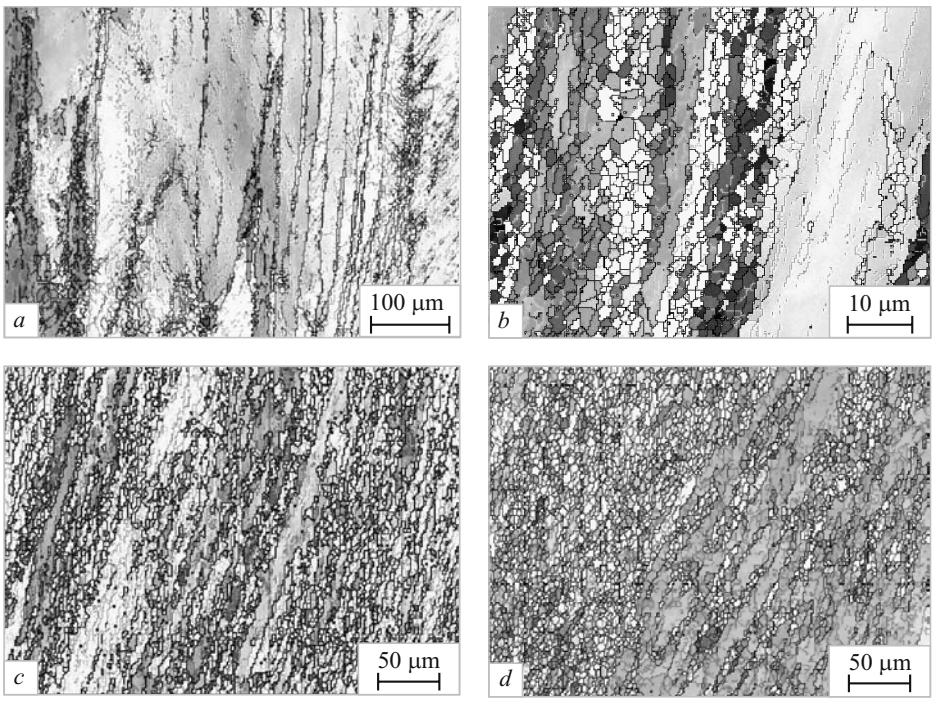

Fig. 4. Maps obtained by EBSD-analysis of the Al – 3% Cu alloy after deformation by the method of ECAP at 250°C: *a*) ε = 1; *b*) ε = 2; *c*) ε = 8; *d*) ε = 12; the gray lines mark the boundaries with mean angle $\theta_m = 5 – 15°$; the black lines mark the boundaries with mean angle $\theta_m > 15°$.

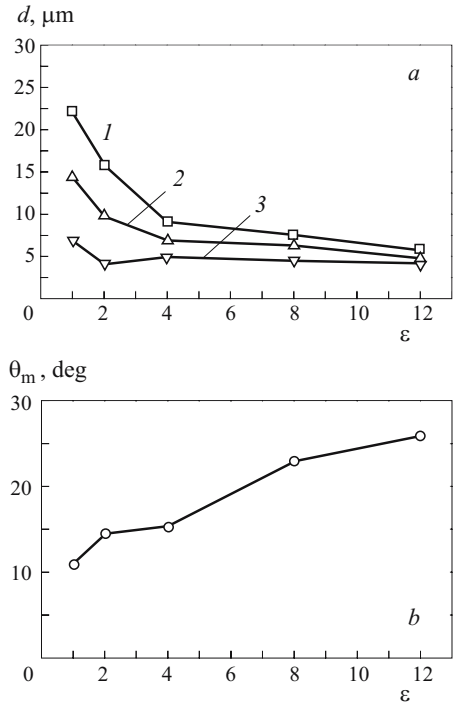

Fig. 5. Dependence of the sizes of crystallites *d* (*a*) and of the mean grain-boundary angle θ_m (*b*) on the degree of deformation by the method of ECAP (t_{def} = 250°C) for the Al – 3% Cu alloy: *1*) width of crystallite bands; *2* and *3*) sizes of crystallites in the longitudinal and transverse directions of the deformation, respectively.

characteristic feature of such band is a "tooth" pattern of the longitudinal LAB.

It has been shown that collision of opposite boundaries causes separation of the bands into strongly elongated grains having a like orientation. At ε ~ 1 a weak subgrain structure develops in the body of initial grains. The angle of SAB is about 1°; a three-dimensional network of SAB develops seldom. In rare cases individual boundaries of subgrains having a favorable orientation for multiple sliding of lattice dislocations in the {111}⟨110⟩ system can be seen inside initial grains. At the same time, well discernible nets of strain-induced boundaries can be seen (Fig. 4*a*) in two different regions. The regions of the first kind lie between extended medium- and large-angle boundaries or between a boundary of this type and an old boundary. Individual elongated boundaries with an angle of about 12° usually lie on primary sliding systems in the direction of the displacement (Fig. 4*a*). We can also detect isolated segments with higher misalignment or even initially large-angle segments arranged over continuous medium-angle boundaries (Fig. 4*a*). If the elongated medium- and large-angle boundaries lie in the vicinity of initial LAB, we can observe a mixed net of SAB and LAB between them (Fig. 4*a* and *b*). It can be seen that the old boundaries in these regions are strongly toothed (Fig. 4*b*). We have also detected (Fig. 4*a*) the presence of the second type of regions in the body of initial grains where two systems of medium-angle boundaries intersect. These regions acquire a spatial net of strain-induced boundaries with angles ranging from low to high values. Inside these two regions we observed fully recrystallized grains surrounded by LAB on all sides. Thus, the Al – 3% Cu alloy deformed with ε ~ 1 acquired recrystallized grains of two different types.

After deformation with ε ~ 2 a developed subgrain structure is observed in the body of the initial grains (Fig. 4*b*). In addition to the prevailing SAB with angle θ < 5° we can see individual fine grains (Fig. 4*b*). A mixed net consisting of SAB and LAB forms between two longitudinal LAB. The mean width of the bands of new crystallites amounts to 16 – 20 μm (Fig. 5*a*). Such boundaries can be quite toothed or relatively straight (Fig. 4*b*). The mean SAB angle in the net is about 5° (Figs. 4*b* and 5*b*); strain-induced boundaries with a mean angle θ ~ 12° and large angles prevail. On the whole, the fraction of LAB increases with growth in the degree of deformation from about 1 to about 2 (Fig. 3) despite

the fact that the fraction of SAB with angles smaller than 5° does not change. A special feature of the Al – 3% Cu alloy is a high fraction of medium-angle boundaries with angles ranging from 10 to 15°.

Upon further deformation the microstructure is divided into recrystallized regions where medium- and large-angle boundaries prevail and nonrecrystallized regions where the net of strain-induced boundaries consists of SAB with angles below 5°. After deformation with $\varepsilon \sim 8$ bands of recrystallized grains alternate with bands of nonrecrystallized structure consisting of recovery subgrains with angles $\theta < 5°$ (Fig. 4*c*). We also observe recrystallized grains of two types, i.e., equiaxial and elongated. New grains with equiaxial shape predominate (Figs. 4*c* and 5*a*). The orientation of neighboring grains in such recrystallized regions differs noticeably. The proportion of elongated grains grouped into chains with close orientation is low.

Further deformation to up to $\varepsilon \sim 12$ leads to an increase in the proportion of recrystallized grains (Fig. 4*d*) surrounded by LAB on all sides and to an increase in the proportion of LAB. At $\varepsilon \sim 12$ the distribution of LAB angles becomes more uniform. The larger part of SAB with angles less than 5° is tied to the subgrain structure in nonrecrystallized regions. Medium- and large-angle angles are typical for recrystallized regions (Fig. 4*d*).

The effect of ECAP on the number of LAB is presented in Fig. 3 and that on the structural parameters of strain-induced crystallites is presented in Fig. 5*a*. The evolution of the width of crystallite bands as a result of collision with LAB is represented by a separate line (curve *1* in Fig. 5*a*). It can be seen that the transverse size of the (sub)grains decreases inconsiderably with growth in the degree of deformation. This size and the width of strongly elongated grains are very close due to the division of elongated (sub)grains oriented in the direction of displacement by transverse SAB that transform continuously into HAB upon growth in the degree of deformation (Figs. 4 and 5).

The data presented in Fig. 5*b* show that the mean grain-boundary angle increases progressively in the whole of the deformation range. The results obtained can be approximated by a linear function of accumulated strain having the form $\Delta\theta \propto 2.2° \times \Sigma\varepsilon$. It can be seen that this level for alloy Al – 3% Cu is about twice lower than for alloy 2219. With growth in the degree of deformation the proportion of the strain-induced LAB increases (Fig. 3). However, the degree of this increase is not high; the proportion of LAB in Al – 3% Cu does not exceed 50% even at $\varepsilon \sim 12$. At high degrees of deformation the alloy acquires a partially recrystallized structure.

DISCUSSION OF RESULTS

The experimental results obtained show that the main mechanism of formation of ultrafine-grained structure in both alloys is CDR. The initial stages of the deformation ensure the formation of a net of small-angle subboundaries, and with growth in the degree of the deformation SAB transform into LAB due to a progressive increase in the SAB angle [18]. However, the phase composition of Al – Cu alloys has considerable influence on the processes of grain refinement.

Alloy 2219. In this alloy the nanoparticles of Al_3Zr serve as effective stabilizers of the SAB net of the grains [19]. As a result, the mobility of the strain-induced SAB decreases, the obvious interaction between subboundaries that consist of dislocations with opposite Burgers vectors is absent, and they undergo mutual annihilation [20, 21]. Three-dimensional nets of immobile subgrain boundaries lie inside old grains upon deformation of degree $\varepsilon \sim 1$. The increase in the grain-boundary angle of isolated segments of strain-induced SAB with respect to the neighbor segments of elongated SAB implies that the main mechanism ensuring growth in the SAB angles with the degree of deformation is local capture of mobile lattice dislocations. Lattice dislocations move across subgrains. Accumulation of mobile lattice dislocations in immobile SAB ensures gradual growth in their angles and thus leads to progressive transformation of SAB into LAB. Al_3Zr dispersoids lower the mobility of LAB due to the Zener force [20] and hinders the grain growth. Consequently, the particles of Al_3Zr play the role of stoppers for all types of strain-induced boundaries in alloy 2219 by preserving the size stability of the newly formed (sub)grains (Fig. 2*a*).

Alloy Al – 3% Cu. The low-alloy Al – 3% Cu alloy does not contain particles hindering the migration of small-angle grain boundaries. The strain-induced SAB possess a high mobility, which leads to their intersection and mutual annihilation [20, 21]. This explains the complexity of the occurrence of both mentioned CDR processes inside the initial grains of the Al – 3% Cu alloy. For this reason only an inconsiderable number of recrystallized grains forms according to these types of CDR. Consequently, the CDR, which can be treated as a uniform process, plays an inconsiderable role in grain refinement in alloy Al – 3% Cu.

In the low-alloy aluminum alloy CDR occurs quite nonuniformly. This is connected with the formation of strain-induced bands after the first deformation pass. The exact mechanism of formation of elongated strain bands separated by large-angle boundaries is being studied [22, 23].

CONCLUSIONS

1. It has been shown that the main mechanism of refinement of structure in Al – Cu alloys in the process of severe plastic deformation is continuous dynamic recrystallization (CDR). A necessary condition for the occurrence of CDR is the presence of stable subboundary nets in the early stages of plastic deformation.

2. Al_3Zr dispersoids in alloy 2219 play the role of effective stoppers, as a result of which the CDR occurs nonuniformly.

3. In the low-alloy Al – 3% Cu alloy a net of small-angle boundaries stabilizes the boundaries of strain bands having large-angle orientation and the elongated medium- and small-angle boundaries. New grains in the low-alloy alloy nucleate as a result of a continuous strain-induced process that occurs nonuniformly.

REFERENCES

1. N. N. Tsuji, S. Okyno, T. Matsura, et al., *Mater. Sci. Forum*, **426**(4), 2667 (2000).
2. F. J. Humphreys, P. B. Prangnell, R. J. Bowen, et al., *Philos. Trans. R. Soc. Lond.*, **357A**, 1663 (1999).
3. R. Z. Valiev, R. K. Islamgaliev, and I. V. Alexandrov, *Prog. Mater. Sci.*, **45**, 103 (2000).
4. A. Golinia, P. B. Prangnell, and M. V. Markushev, *Acta Mater.*, **48**, 1115 (2000).
5. Y. Iwahashi, Z. Horita, M. Nemoto, and T. G. Langdon, *Acta Mater.*, **46**, 3317 (1998).
6. Y. Iwahashi, Z. Horita, M. Nemoto, and T. G. Langdon, *Acta Mater.*, **45**, 4733 (1997).
7. K. Nakashima, Z. Horita, M. Nemoto, and T. G. Langdon, *Acta Mater.*, **46**, 1589 (1998).
8. P. J. Apps, J. R. Bowen, and P. B. Prangnell, *Acta Mater.*, **51**, 2811 (2003).
9. W. Q. Cao, A. Godfrey, and Q. Liu, *Mater. Sci. Eng.*, **361**, 9 (2003).
10. S. D. Terhune, D. L. Swisher, K. Oh-ishi, et al., *Metall. Mater. Trans.*, **33A**, 2173 (2002).
11. S. Ferrase, V. Segal, K. Hartwig, and R. Goforth, *Metall. Mater. Trans.*, **28A**, 1047 (1997).
12. A. Belyakov, T. Sakai, H. Miura, and K. Tsuzaki, *Philos. Mag.*, **81**, 2629 (2001).
13. A. Belyakov, T. Sakai, and H. Miura, *Mater. Trans. JIM*, **41**, 476 (2000).
14. I. A. Mazurina, O. Sh. Sitdikov, and R. O. Kaybyshev, *Phys. Metal. Metall.*, **94**, 413 (2002).
15. O. Sh. Sitdikov, R. O. Kaybyshev, I. M. Safarov, and I. A. Mazurina, *Phys. Metal. Metall.*, **92**, 270 (2001).
16. R. Kaibyshev, K. Saytaeva, F. Musin, and Y. Motohash, in: *Hot Deformation of Aluminum Alloys III*, TMS, USA (2003), p. 365.
17. G. Thomas and M. J. Goringe, in: *Transmission Electron Microscopy of Materials*, Wiley, New York (1983), pp. 99 – 119.
18. S. Courdet and F. Montheillet, *Acta Mater.*, **51**, 2685 (2003).
19. J. Humphreys and M. Hatherly, in: *Recrystallization and Related Annealing Phenomena*, Pergamon Press, Oxford, UK (1996), p. 493.
20. O. Sitdikov and R. Kaibyshev, *Mater. Sci. Eng.*, **328**, 147 (2002).
21. M. Biberger and W. Blum, *Philos. Mag. A*, **65**, 757 (1992).
22. A. Cholinia, F. J. Humphreys, and P. B. Prangnell, *Acta Mater.*, **50**, 4461 (2002).
23. M. A. Shremel, in: *The Strength of Alloys, Part 1, Lattice Defects*, MISIS, Moscow (1999).